MAPPING MODERATE REDSHIFT CLUSTERS*

BY R.G. CARLBERG[1,12], H.K.C. YEE[1], ERICA ELLINGSON[2], C.J. PRITCHET[3], ROBERTO ABRAHAM[4], TAMMY SMECKER-HANE[4], J.R. BOND[5], H.M.P. COUCHMAN[6], D. CRABTREE[4], D. CRAMPTON[4], TIM DAVIDGE[11], D. DURAND[4], S. EALES[1], F.D.A. HARTWICK[3], J.E. HESSER[4], J.B. HUTCHINGS[4], N. KAISER[5], C. MENDES DE OLIVEIRA[7], S.T. MYERS[8], J.B. OKE[4], M.A. RIGLER[4], D. SCHADE[9], AND M. WEST[10]

[1]Department of Astronomy, University of Toronto, [2]Department of Astronomy, University of Colorado, [3]Department of Physics and Astronomy, University of Victoria, [4]Dominion Astrophysical Observatory, National Research Council, [5]Canadian Institute for Theoretical Astrophysics, University of Toronto, [6]Department of Astronomy, University of Western Ontario, [7]Institut d'Astrophysique, Paris, [8]Department of Astronomy, California Institute of Technology, [9]Institute of Astronomy, Cambridge University, [10]Sterrewacht, Leiden University, [11]Gemini Project Office, University of British Columbia, [12]Department of Astronomy, University of Washington

(Received July 10, 1993; revised September 14, 1993)

ABSTRACT

To test whether clusters of galaxies have rising mass-to-light ratios at large radii and to estimate the amplitude of the density fluctuation spectrum on the scale of $10h^{-1}$ Mpc, the Canadian Network for Observational Cosmology (CNOC) cluster collaboration is obtaining Multi-Object Spectrograph velocities and two colour photometry for a sample of $\simeq$1000 cluster galaxies and $\simeq$2000 field galaxies in a $5h^{-1}$ Mpc neighbourhood of high X-ray luminosity clusters at $z \simeq 0.3$. X-ray selection of the cluster sample picks out objects on the basis of the depth of their potential well, and is insensitive both to projection effects and to galaxy biases. The galaxy data set, with selection controlled using automated photometry, automated mask design, spectral selection modelling, and accurate velocities, will be the best available at any redshift for our tests. Measuring mass-to-light ratios (M/L) at large radii requires a statistical removal of field galaxies projected into a redshift space of the cluster. This can be done relatively accurately for moderate redshift clusters, using the large number of foreground and background galaxies. The CNOC sample also provides a sensitive test of the density fluctuation spectrum on cluster scales. The 30 or so redshifts available in each of three clusters gives an average velocity dispersion of about 1000 km s^{-1} which indicates that the σ_8 normalization parameter is in the range of $0.6 \lesssim \sigma_8 \lesssim 0.9$.

RÉSUMÉ

Afin de déterminer les rapports masse-luminosité à la périphérie des amas de galaxies et l'amplitude du spectre des fluctuations de densité sur une échelle de $10h^{-1}$ Mpc, le Groupe canadien de Recherche en Cosmologie Observationnelle (GCRCO) a entrepris une étude des vitesses radiales (mesurées avec le spectrographe multi-objet) et de la photométrie en deux couleurs de quelques

*Invited paper at the meeting of the Canadian Astronomical Society, held at the University of Victoria, June 1–5, 1993, commemorating the 75th anniversary of the start of scientific observations with the Plaskett Telescope of the Dominion Astrophysical Observatory.

1000 galaxies dans des amas et de 2000 galaxies dans un rayon de $5h^{-1}$ Mpc autour des amas qui sont d'intenses sources de rayons X à $z = 0.3$. La sélection des amas basée sur leur émission de rayons X dépend de la profondeur du puits de potentiel et n'est donc pas influencée par des effets de projection ou des biais envers certaines galaxies. L'ensemble des données recueillies sur ces galaxies, dont la sélection repose sur la photométrie et la fabrication de masque automatisées, le modelage de la sélection spectrale et des vitesses radiales précises, sera celui qui se prêtera le mieux à plusieurs tests cosmologiques. En effet, le rapport masse-luminosité d'amas de galaxies peut être mesuré s'il est possible d'éliminer les galaxies dans le champs d'après leur redshift, et cette procédure statistique, qui peut être utilisée pour les amas situés à des redshifts modérés, requiert un grand nombre de galaxies en avant-plan et en arrière-plan. L'échantillon du GCRCO peut aussi servir à tester le spectre des fluctuations de densité à l'échelle de ces amas de façon très sensible. Les quelques 30 redshifts recueillis pour chacun des trois amas observés jusqu'à maintenant donnent une dispersion de vitesse moyenne d'environ 1000 km s^{-1}. Ce résultat indique que la valeur du paramètre de normalisation σ_8 se situe entre 0.6 et 0.9.

LS

1. Introduction. The mean mass density of the universe is a fundamental cosmological parameter for which there are two relatively distinct values implied by observations at two different length scales. We define, as usual, $\Omega = \rho/\rho_0$, where ρ is the observed mean mass density, and ρ_0 is the mean mass density required to "close" the universe. Large scale streaming velocities find that $\Omega^{0.6}/b \simeq 1$ (Bertschinger *et al.* 1990, Kaiser *et al.* 1991, Strauss *et al.* 1992), where b is the poorly known bias parameter. For $b \simeq 1$ the streaming velocities are consistent with $\Omega = 1$, as predicted by inflationary cosmology (Guth 1981, Bardeen *et al.* 1983). Measurements from somewhat smaller scales, where virialized motions dominate, favour $\Omega \simeq 0.2$ (*e.g.* Kent and Gunn 1982, Davis and Peebles 1983, Bean *et al.* 1983). Taken together the two measurements suggest that large clusters of galaxies may have dark matter haloes that extend far beyond the bulk of their visible galaxy distribution. Furthermore, there is evidence from n-body simulations that a segregation of galaxies and dark matter can develop even within the dissipationless clustering that leads to the buildup of a large cluster (West and Richstone 1988, Carlberg and Couchman 1989, Carlberg *et al.* 1990, Carlberg and Dubinski 1991). Individually the galaxies accurately measure the mass inside their orbits, but their distribution as a population can be more centrally concentrated than the total mass distribution. The primary goal of our observations is to establish whether the mass-to-light ratio of clusters rises beyond the virial radius.

At the present time the best data for measuring cluster masses at large radii come from galaxy redshifts. The difficulty in interpreting a redshift map is that it is impossible to distinguish between a cluster galaxy orbiting with a line-of-sight velocity of, say, 2000 km s^{-1} and a field galaxy with no peculiar velocity situated $20h^{-1}$ Mpc from the cluster. (Here h is the Hubble constant in units of 100 km s^{-1} Mpc^{-1}.) The normal procedure for virial mass measurements is

to terminate the analysis where the projected cluster blends into the field. This paper presents a straightforward method which treats the field galaxies as an asset which is used to remove statistically the background contamination in the cluster redshift map. For samples of a few thousand galaxies, spread over about 10 clusters, the method is shown to test reliably for the presence or absence of extended mass around clusters, as expected in $\Omega = 1$ or $\Omega = 0.2$ universes, respectively.

The statistical requirements for measuring the mass profile motivate the design of our observations. A critical assumption of the mass estimation method is that the cluster has no nonspherical structure beyond linear gradients in density front to back and side to side. However, clusters are known to be triaxial, and are embedded in a rich mixture of surrounding large scale structure and have the further difficulty that the sampling efficiency is likely to vary over large angles on the sky, such as the 30° spanned by the Coma data. The cluster asymmetries can be averaged out using a small sample. Clusters at moderate redshifts, $z \simeq 0.3$, can be selected from X-ray surveys, the galaxies within them can be sampled with good statistical control, and there are sufficient foreground and background galaxies that the projection corrections are well determined. This redshift range is also accessible to other observational techniques which can be used to measure the mass profile, in particular weak gravitational lensing and X-ray observations, although so far these are confined to the inner $1h^{-1}$ Mpc of a cluster. These other observations will provide constraints on the relations between the virial temperatures of the galaxy orbits, the X-ray gas, and the dark matter. Moderate redshift clusters are also a superb match to the observational capabilities of Canada France Hawaii Telescope (CFHT), where a single Multi-Object Spectrograph (MOS, Crampton *et al.* 1993, LeFèvre *et al.* 1993, Morbey, C.L. 1992) field subtends $\simeq 2.5h^{-1}$ Mpc and more than 100 galaxy spectra can be acquired in two hours at the magnitude limit of our survey.

The volume density of high velocity dispersion clusters is a sensitive indicator of the amplitude of density fluctuations on cluster scales, parameterized by σ_8, the fractional mass variance in randomly placed spheres of 8 h^{-1} Mpc radius. The bias parameter, $b = 1/\sigma_8$, is essential for interpreting the large scale flow velocities, and many other aspects of the relations of luminous galaxies to the underlying dark mass fluctuations. To overlap a measurement of σ_8 with our mass profile study, we must select a sample that is likely to have high velocity dispersions and whose volume density can be well defined. Accordingly, the clusters are selected to be an X-ray flux limited sample with high luminosities. The number density of clusters is a strong function of the "peak height", which is directly related to the cluster velocity dispersion, with a normalization parameter which is the amplitude of the density fluctuation spectrum on cluster scales, σ_8. The value of σ_8 is vigorously debated. It has been estimated from optically

selected cluster samples (Frenk *et al.* 1990, White *et al.* 1993) and cluster X-ray luminosity and temperature functions (*e.g.* Evrard and Henry 1991, Kaiser 1991) who argue that $\sigma_8 \simeq 0.6$, but a somewhat different theoretical calibration and allowance for redshift evolution in the sample finds σ_8 in the 0.7 to 0.9 range (Bond and Myers 1992). Our sample is effectively selected on the basis of the dark matter potential well, and we use the galaxies only to gauge the depth of the well. Our initial data allow us to put an interesting new limit on σ_8.

This paper discusses the basic analysis which will be used for cluster mass profiles and σ_8 measurements. The reader is referred to Yee *et al.* (1993) for a discussion of the innovative observational techniques which ensure statistically uniform selection of galaxies, achieve a velocity accuracy of $\lesssim$150 km s^{-1} as is necessary for the study of cluster dynamics, and yield 10–20 $m_R \leqq 21.5$ redshifts per dark hour with the CFHT.

2. Cluster Mass Profiles. Luminosity segregation has long been recognized to be a possibility within clusters, with the galaxies being more concentrated to the centre than the dark matter. There is no evidence for or against such a segregation, given the relatively small radial range of the data (The and White 1986, Merritt 1987). The discrepancy between cluster virial Ω values, and the Ω values obtained from large scale streaming, which are measured on scales only three times as large, suggests that the excess mass of $\Omega = 1$ over $\Omega \simeq 0.2$ may be located on the outskirts of clusters (if it can undergo gravitational clustering). The study of the Coma cluster by Kent and Gunn (1982) had about 300 cluster velocities within 3° of the centre, from which they concluded that a light-traces-mass model was entirely compatible with the available data, but that a rising M/L ratio could not be ruled out. A test of whether M/L rises with radius depends on getting many velocities at as large an angular radius as possible, in which case the projection of foreground and background objects into the cluster's redshift space poses a severe problem.

The observational situation for the Coma cluster is illustrated in figure 1 using ZCAT redshifts (Huchra *et al.* 1992) for $m_B \leqq 16.5$ galaxies within 15° and 5000 km s^{-1} of the Coma cluster centre. This dataset is a hodgepodge, and *is not uniform across the cluster* (van Haarlem *et al.* 1993) and will not give reliable masses. A more uniform sample limited at $m_B = 14.5$ does not have enough cluster galaxies to be useful beyond about 2°. The magnitude limit of 16.5 is chosen primarily to give a sample size comparable to our survey. The velocities have been folded about the centre of velocity and plotted against angular separation from the centre of the cluster in order to average over the surrounding large scale structure as much as possible. The average and root-mean-square (RMS) velocities rise to nearly half of the 5000 km s^{-1} range, indicating a severe field contamination, even at angles as small as 3°.

A simple approach to "decontaminate" the cluster redshift map is to take advantage of the vast number of galaxies which are in the surrounding field but which are relatively unmoved by the cluster. Under the assumption of uniform sampling, the galaxy density at large radii can be used statistically to estimate the contamination through the cluster. For the illustrative application to the Coma cluster the background correction is based on the redshift map density of galaxies at large angles, 10° to 15°. For moderate redshift clusters we shall use the galaxies in front of and behind the cluster in redshift space. In this paper the subtraction will be done in bins of $[\Delta v, \theta]$, but the same technique can be implemented within a maximum likelihood model. The results of the field subtraction are shown in figure 2. Bins of 500 km s^{-1} and 1° were used. The velocity profile is not expected to be useful for a serious mass estimate because of non-uniform sampling of the sky and single clusters cannot give reliable mass profiles. Figure 2 does show that the background subtraction technique qualitatively works on real world data. The quantitative accuracy for mass estimation is assessed with simulation data.

The ability of the mass estimation method to discriminate between low and high Ω universes can be tested using results from n-body simulations. Two simulations in $100h^{-1}$ Mpc boxes are used, one with $\Omega = 0.2$, the other with $\Omega = 1$. In both cases the initial conditions were 128^3 particles perturbed with a standard Cold Dark Matter (CDM) model evolved until $\sigma_8 = 1$ for $\Omega = 1$ and $\sigma_8 = 3$ (in this patch) for $\Omega = 0.2$. These parameters create a large cluster in each simulation with a velocity dispersion of about 1000 km s^{-1}. Samples of particles are drawn from the particles within $15h^{-1}$ Mpc of the cluster centre, and within 5000 km s^{-1} of the line-of-sight velocity (including Hubble flow) of the cluster centre of velocity. The $\Omega = 0.2$ model is a light-traces-mass model, so the sample of 2000 particles is drawn at random. To be realistic, the tracers in the $\Omega = 1$ model must indicate a virial mass for the cluster about 0.2 of the true virial mass. Accordingly the sample was created from a random sample of the particles which were in $\rho \gtrsim 1000\rho_0$ regions at $z = 3$.

Figure 3 shows the corrected $[\Delta v, \theta]$ maps for the two simulations and the mass profiles, real space measurements (asterisks) and estimates from the decontaminated redshift map (triangles on the solid line). The clusters are observed from the three coordinate directions to help average over the strong surrounding structure. The masses are estimated using the projected mass estimator (Bahcall and Tremaine 1981),

$$M_P(< r_p) = \frac{S\sigma_1^2(r_p)r_p}{\pi G}, \tag{1}$$

where S is the orbit shape coefficient, which ranges from 16 to 32 for isotropic to completely radial orbits, and r_p is the projected distance from the centre of the

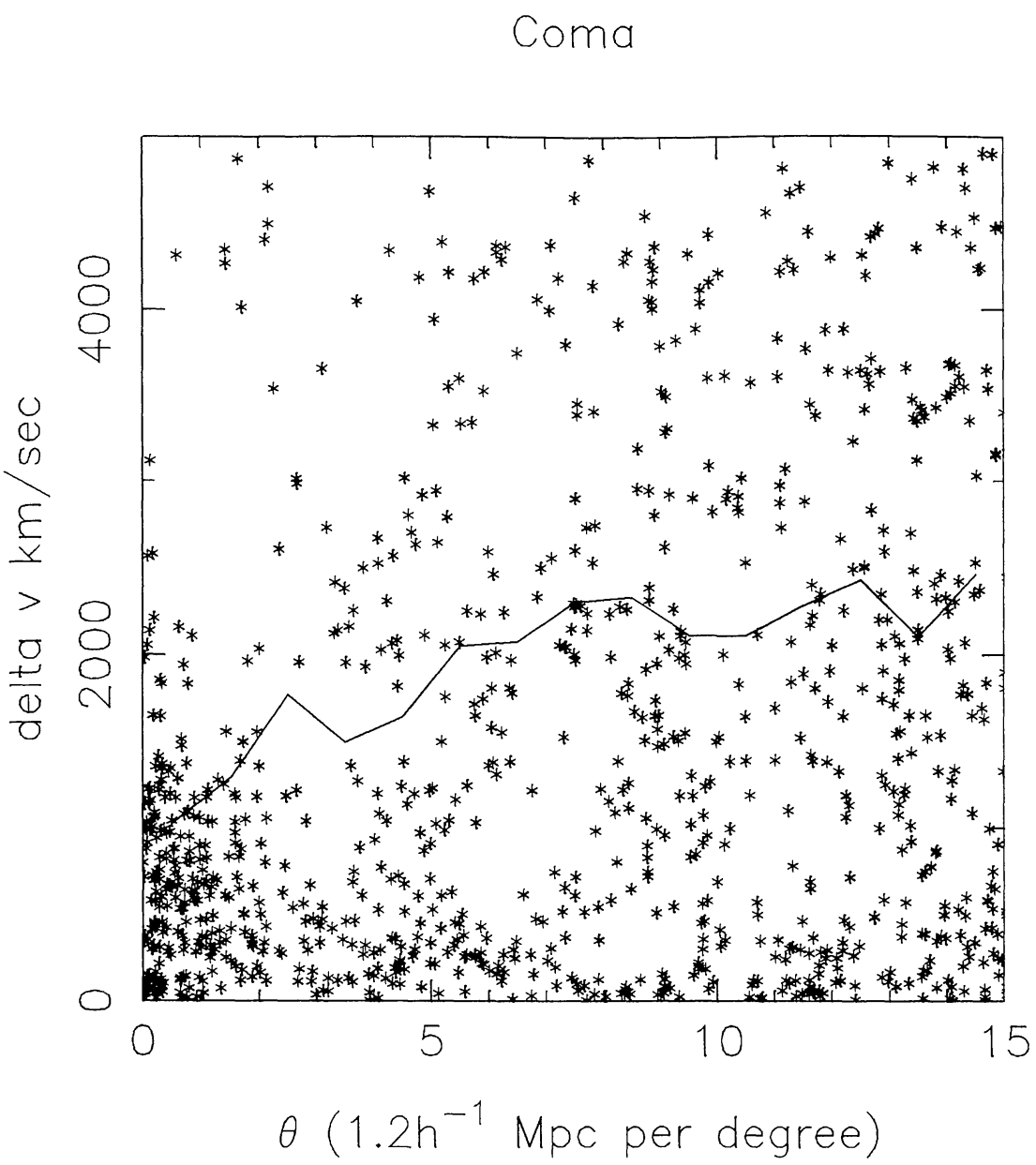

FIG. 1—The ZCAT distribution of velocities in the Coma field ($m_B \leqq 16.5$) plotted against angular separation folded about the central redshift, which helps to smooth over surrounding large scale structure, and eliminates linear selection gradients. The line gives the RMS velocity in this background contaminated sample. Note that the ZCAT sample is made from several heterogeneous surveys of varying depth across the cluster, and is far from the uniform survey which is essential for mass estimates at large radii.

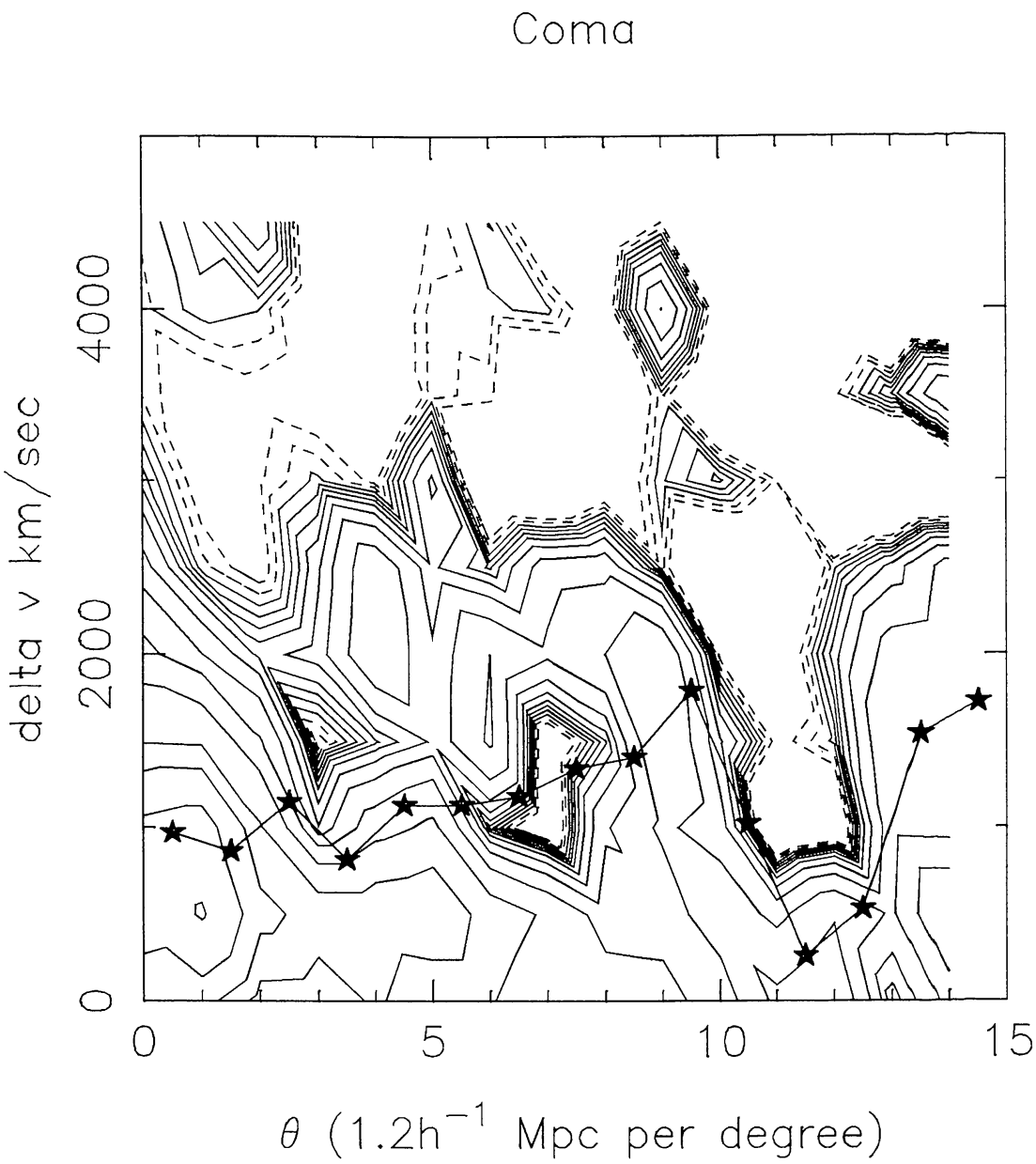

FIG. 2—The background subtracted redshift map density distribution for the Coma field. Contours of density are plotted at intervals of 0.2 in $\log_{10}$, except for the bottom five contours, which are linear between 0.4 and −0.4. The bins are 500 km s^{-1} by 1°. The solid line shows the estimated velocity dispersion. Note the effective removal of projected galaxies at large velocities. Comparison with maps drawn from *n*-body data indicates that this map is relatively free of problems to a distance of 5°. The errors in this map are dominated by the nonuniform sampling of the cluster.

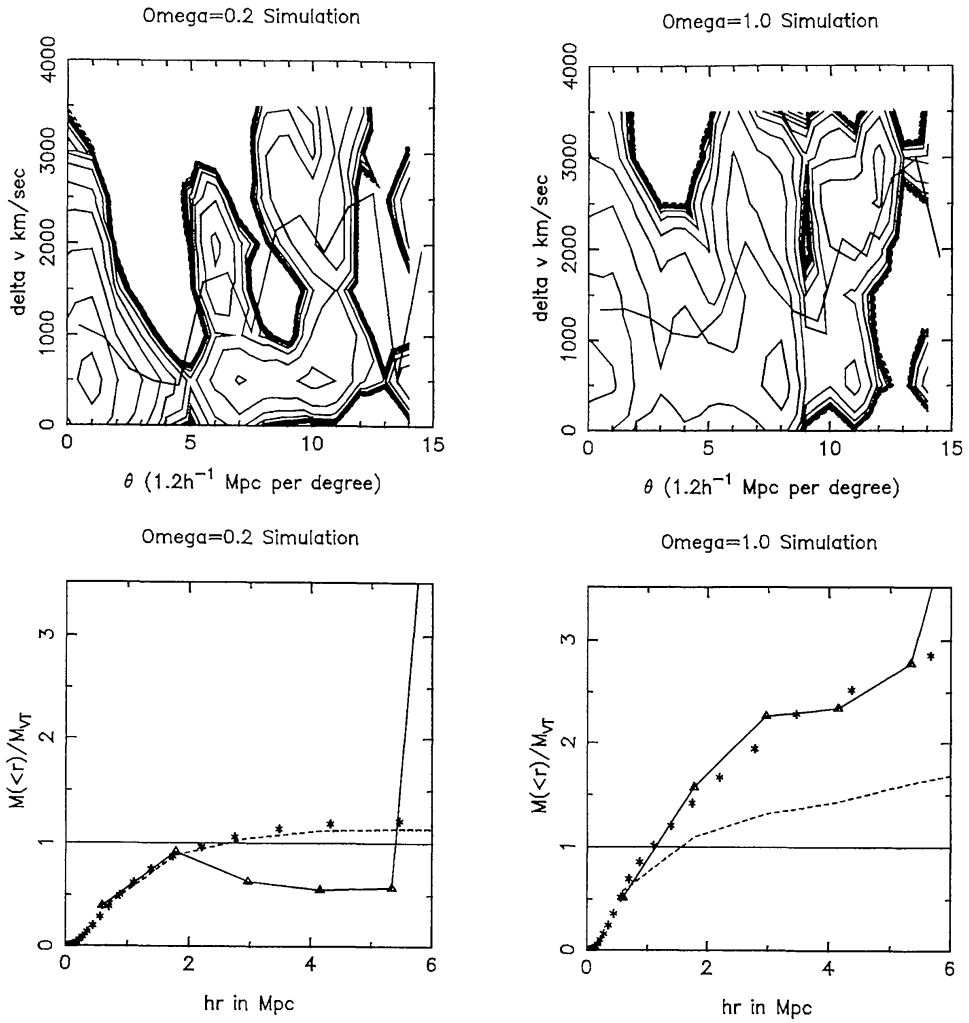

FIG. 3—N-body tests of the contamination correction and mass estimation for a light-traces-mass, $\Omega = 0.2$ simulation (left side plots) and a biased $\Omega = 1$ simulation in which the tracers indicate a cluster virial mass equivalent to $\Omega_{VT} \simeq 0.2$ (right side plots). The plots are done for the single largest cluster found in the two simulations. In the absence of cluster averaging there is no possibility of distinguishing the difference between the $\Omega = 0.2$ and $\Omega = 1$ models, because the velocity fields are dominated by local asymmetries. More n-body simulations are planned (requiring about a cpu-year of computing time on a modern workstation) to allow a representative averaging over simulated clusters, but in the meantime the clusters are averaged over the three independent projections (which does not suppress local structure as well as three separate clusters would). The simulation data are scaled to the distance of the Coma cluster and similar numbers of particles are used (about 400 in the cluster with a total of about 2000). The top plots show corrected density contours in the $[\Delta v, \theta]$ plane. The method works well until the tracer density becomes comparable to the noise, in which case characteristic "islands" and "peninsulas" appear. In both cases the data are judged to be reliable to about 5°. The bottom plots show the mass estimator. The dashed lines indicate the enclosed light, which for the light-traces-mass model on the left nicely traces the mass enclosed (shown by asterisks) obtained by directly counting particles in spheres in the full three-dimensional data set.

cluster. The velocity ellipsoid shapes are known from cosmological simulations to be mildly radial, but as a conservative choice we use $S = 16$. The values for $\sigma_1(\theta)$ are derived from the decontaminated redshift map of figure 2. To reduce graininess due to binning, the RMS velocities are accumulated for each bin, rather than simply being placed at the centre of the bin. The projected mass is normalized to the virial mass, which is calculated using all galaxies within 3000 km s^{-1} and 3° of the centre for the cluster,

$$M_{VT} = \frac{3\pi\sigma_{1,RMS}^2}{2G\langle 1/r_p\rangle}. \tag{2}$$

The tests of the decontamination and mass estimation procedures using simulation data shown in figure 3 build confidence that the method makes efficient use of the data to estimate cluster masses. A data set of 400 cluster velocities and about 2000 total is sufficient to signal clearly the presence or absence of extended dark haloes, out to a radius of about $6h^{-1}$ Mpc. It is also evident that the maps develop "islands" and "peninsulas" at large Δv and r_p, which are a clear indication that the noise is overwhelming the signal. In the $\Omega = 0.2$ model of figure 3 the cleaned integrated light distribution does a remarkable job of following the integrated mass distribution, indicating that the decontamination works extremely well on integral quantities. Most importantly, for both the $\Omega = 1$ and $\Omega = 0.2$ data sets the estimated mass profile is close to the true mass distribution. The radial bins are 1° here, although averaging over 2° gives a somewhat improved $M(< r)$ estimate, particularly for the $\Omega = 0.2$ case. Because the three projections are not independent, the effective amount of data will be somewhat smaller than the 3×400 cluster particles selected in each case. It appears safe to conclude that with a sample of about 1000 cluster galaxies, spread over a number of clusters, it will be possible to measure the mass profile of the cluster, with a statistical accuracy nearly at the $\sqrt{N}$ level of the amount of data at large radii.

Simulating only two clusters serves to illustrate the effectiveness of the method, but it does not give an indication of the errors. Ultimately a sample of 100 or so realizations of these two models will be studied to better determine the errors of mass determination, estimate the effect of substructure in velocity distributions on velocity dispersion estimates, and to calibrate the relation between observed velocity dispersion and the volume density of clusters, as discussed below using an analytic theory.

3. The Density Fluctuation Spectrum Amplitude. The amplitude of the density fluctuation spectrum, $P(k)$, is conventionally given by σ_8, defined as the linear extrapolation of the mass variance in a sphere of $8h^{-1}$ Mpc radius measured at the current epoch. In the galaxy population the variance of number density

is equal to 1, within the errors; hence the bias parameter is $b = 1/\sigma_8$. For the "classical" CDM spectrum, $\sigma_8 \simeq 0.4$ (Davis *et al.* 1985) if $\Omega = 1$ and galaxies accurately represent the pairwise velocities of the dark matter population. The large scale streaming velocities are so much higher than those which a $\sigma_8 = 0.4$ model predicts, that such a low σ_8 has long been ruled out. Furthermore, the large scale streaming velocities indicate $\Omega^{0.6}/b \simeq 1$, so that a knowledge of σ_8 can be combined into an estimate of Ω. The COBE measurement of temperature fluctuations in the cosmic background radiation (Smoot *et al.* 1992), when extrapolated with the $n = 1$ CDM spectrum, predicts that $\sigma_8 \simeq 1.2$ (Wright *et al.* 1992, for a quadrupole amplitude of 15 μK); therefore measurement of σ_8 sets a strong constraint on the shape of the spectrum.

Clusters contain a small fraction of the mass of the universe, meaning that they form from relatively rare perturbations in the extreme tail of the probability distribution. Therefore the number of clusters per unit volume is a sensitive indicator of the amplitude of the perturbation spectrum. As shown below, a factor of two variation in σ_8 changes the number density of clusters by two orders of magnitude. Clusters offer the considerable benefit that they can be viewed as a direct sample of the dark matter, with galaxies simply being a thermometer of the cluster velocity dispersion. Much of the argument over clusters and the density fluctuation spectrum comes from optically selected clusters, which are subject to projection effects which artificially increase the apparent galaxy richness of clusters.

Clusters can be selected from X-ray surveys, which are nearly ideal for our purposes, in that objects are found on the basis of the depth of the potential well and projection overlap of clusters in X-rays is small. The EMSS (Einstein Medium Sensitivity Survey) serendipitous X-ray survey of Gioia *et al.* (1990) (see also Henry *et al.* 1992) has a low enough flux limit to find many luminous clusters at moderate redshifts. Of particular interest are the most luminous clusters, those with X-ray luminosities greater than 4×10^{37} watts, for which several X-ray luminosity function studies have claimed a strong evolution in numbers between $z = 0$ and $z \simeq 0.3$ (Edge *et al.* 1990, Henry *et al.* 1992). Moreover such clusters are most likely to have a high velocity dispersion. Selecting clusters with $z > 0.18$, X-ray luminosities greater than 4×10^{37} watts, and X-ray fluxes greater than 5×10^{-16} W m^{-2} (to ensure inclusion in the ROSAT survey), and in the declination range of $-5°$ to $+40°$ (convenient for long CFHT exposures) gives the sample in Table I.

The expected volume density of clusters as a function of σ_8 can be calculated using the Press-Schechter (1974) theory, which has been shown to be an excellent predictor of the numbers of haloes found in n-body simulations (Efstathiou *et al.* 1988, Carlberg and Couchman 1989). The number of haloes in the range of velocity dispersion σ_v to $\sigma_v + d\sigma_v$ is

TABLE I
THE CLUSTER SAMPLE

Designation of cluster	Redshift	X-ray luminosity 10^{37} W	X-ray flux 10^{-16} W m^{-2}
MS0015.9 +1609	0.540	14.31	11.60
MS0302.7 +1658	0.424	4.99	6.54
MS0440.5 +0204	0.190	4.00	25.92
MS0451.5 +0250	0.202	6.96	39.92
MS0451.6 –0305	0.547	25.10	10.75
MS0839.8 +2938	0.194	5.33	33.17
MS0906.5 +1110	0.180	5.75	41.56
MS1006.0 +1202	0.221	4.80	23.04
MS1224.7 +2007	0.327	4.59	10.08
MS1333.3 +1725	0.460	5.39	6.00
MS1455.0 +2232	0.259	15.98	55.85
MS1512.4 +3647	0.372	4.80	8.15
MS1621.5 +2640	0.426	4.52	5.87

$$n(\sigma_v)d\sigma_v = \frac{9c_v^3 H_0^3}{4\pi\sqrt{2\pi}} \frac{(1+z)^{3/2}}{\sigma_v^4} \frac{d\ln\sigma(M)}{d\ln\sigma_v} \nu e^{-\nu^2/2} d\sigma_v, \quad (3)$$

where $\nu = 1.68(1+z)/(\sigma(M)\sigma_8)$ and we have assumed that $\Omega = 1$. The mass variances, $\sigma(M)$, are calculated from the CDM spectrum. Masses are related to line of sight velocity dispersions as $\sigma_v = c_v H_0 R(1+z)^{1/2}$, where $M = 4\pi\rho_0 R^3/3$. The constant c_v is not well defined, and will be the subject of a large Monte Carlo n-body study. The spherical collapse of a top-hat sphere gives $c_v = 1.18$ (White and Frenk 1991). However, examination of the largest collapsed peaks in the n-body simulations gives $c_v = 1.10$, which we shall adopt (see also Bond and Myers 1993). The tracer population in the cluster of the $\Omega = 1$ model has a considerably lower velocity dispersion, corresponding to $c_v = 0.85$, but this single particle velocity bias is best handled in conjunction with an indication of the mass profile at large radii. A conservative value for the likely velocity bias in clusters is adopted, $b_v = 0.9$, that is, a 10 per cent reduction of the galaxy RMS velocity from the dark matter values (Carlberg and Dubinski 1991).

The solid angle covered by the EMSS sample above our flux limit and in our range of declination is estimated to be 223 square degrees (Henry *et al.* 1992), and the total co-moving volume between $z = 0.18$ and $z = 0.54$ is $3.3 \times 10^7\ h^3$ Mpc^3, for $q_0 = 0.5$. Lower values of the deceleration parameter q_0 give larger volumes. The range of densities is estimated on the basis that there is at least one cluster in this volume, and no more than 12. The predicted volume densities for

TABLE II
CLUSTER VELOCITY DISPERSIONS

Designation of cluster	Redshift	N_c	σ_v km s^{-1}	68% confidence
MS0451.5 +0250	0.2015	24	1097	984–1252
MS0839.8 +2938	0.1924	32	939	796–1071
MS1224.7 +2007	0.3250	29	837	756–931

all clusters with dispersions greater than a given value is the integral of equation (3) from σ_v to infinity.

Preliminary velocity dispersions of three of the clusters are reported in Table II, and have been subjected to a variety of statistical tests (Bird and Beers 1993) for credibility. Eventually we shall obtain about 150 velocities per cluster, thereby greatly improving the statistical accuracy of the dispersions, and allowing clear separation of neighbouring groups. The cluster MS0839+29 has a gap of nearly 600 km s^{-1} in its velocity histogram, which is statistically significant in comparison to a Gaussian (which cluster velocity distributions are not expected to be). Eliminating this gap, and a second smaller one which becomes significant after the first velocity substructure is dropped, reduces the velocity dispersion to about 400 km s^{-1} for this cluster, which would be unusually small, given its X-ray luminosity (Edge and Stewart 1992). Dropping this cluster from the sample would make little difference to either the volume or the average velocity dispersion displayed in figure 4. The highest redshift cluster can be used to put a lower limit on figure 4. The cluster MS1224+20 has a velocity dispersion of 840 km s^{-1} at $z = 0.325$. The co-moving volume from $z = 0.18$ is $1.3 \times 10^8 h^{-3}$ Mpc^3. The lower limit point is plotted with no allowance for velocity bias, which is inconsistent with clusters having extended dark matter haloes.

The implications of this small sample for σ_8 are shown in figure 4. The three clusters have been averaged and $b_v = 0.9$ is adopted. The lower limit is for the single highest redshift cluster, MS1224+20, which has a velocity dispersion of 840 km s^{-1} with the volume is that between our lowest allowed redshift $z = 0.18$ and the cluster redshift, 0.327. We tentatively find that the value of σ_8 is constrained to be in the range of 0.6 to 0.9, which is somewhat higher than found by the studies of the evolution of the X-ray luminosity function (Evrard and Henry 1991, Kaiser 1991, Henry *et al.* 1992) but similar to Bond and Myers (1992). Our σ_8 value combined with the COBE result (Wright *et al.* 1992) is sufficient to argue either that $P(k)$ must have relatively more long wave power than CDM, as suggested by IRAS galaxy surveys (Saunders *et al.* 1991), or that

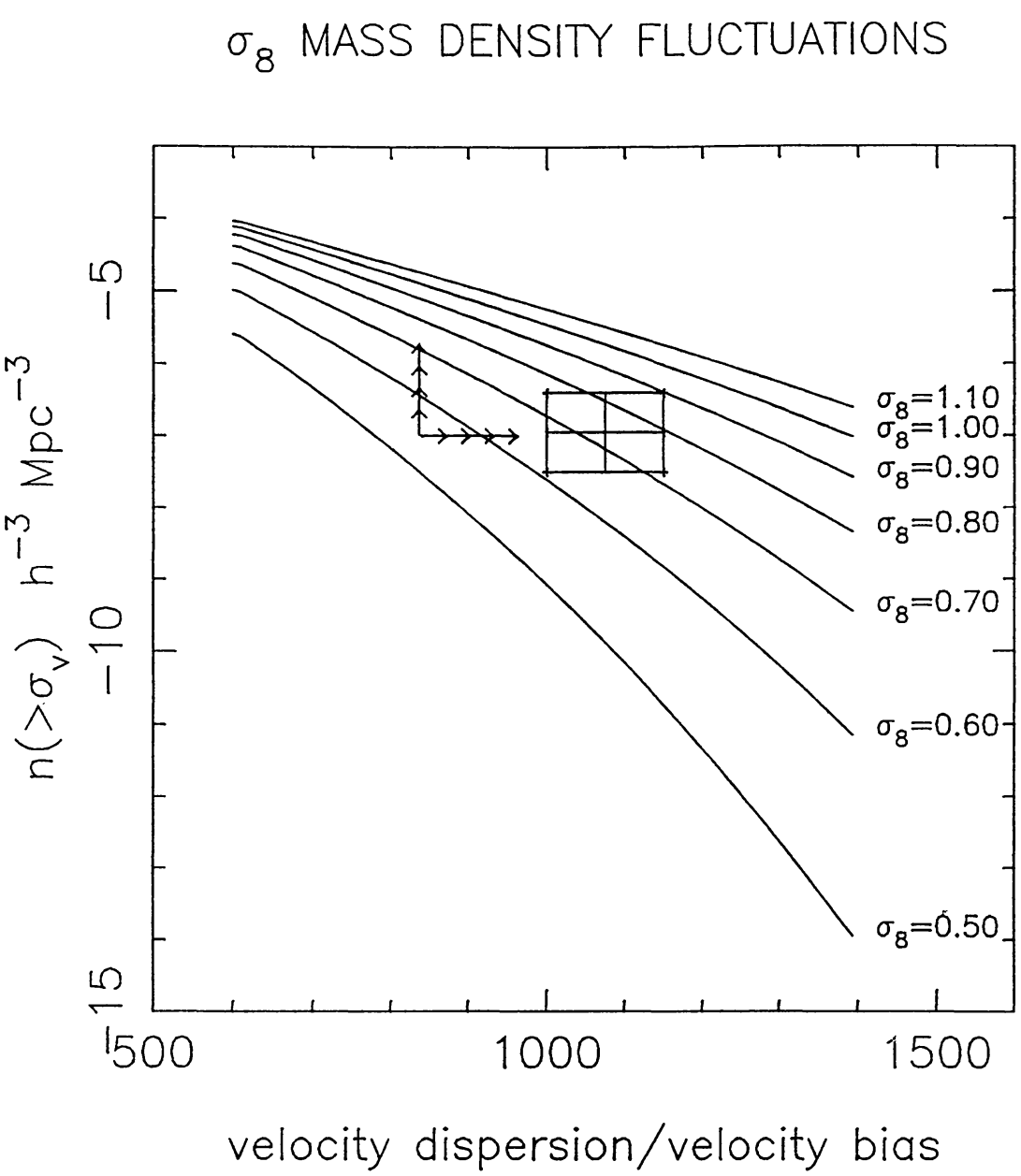

FIG. 4—The volume density of clusters greater than a specified velocity dispersion at $z = 0.3$. The theoretical curves are labelled with their normalized σ_8 values. Note that a factor of two change in σ_8 gives two decades of change in the volume density. The data constraints shown are preliminary results based on three clusters with 30 redshifts each. The lower limit is for the volume enclosed by the highest redshift cluster, MS1224+20, plotted with $b_v = 1$. The error box lower limit assumes one cluster with a dispersion of 950 km s^{-1} in the redshift range 0.18 to 0.54; the upper limit assumes all 12 are in this range. The lower limit uses $b_v = 1$, and the combined data use $b_v = 0.9$.

there are extra sources of variance in the cosmic background radiation (such as primordial gravitational waves). The most significant aspect of this result is a relatively convincing demonstration, based entirely on X-ray selection and velocity dispersion measurements, that the value of σ_8 is in the range of 0.6 to 0.9, and therefore the bias factor, b, is 1.6 to 1.1. When our result is combined with the streaming velocity result, $\Omega^{0.6}/b \simeq 0.7$ (Kaiser *et al.* 1991. Strauss *et al.* 1992), it implies that the large scale value of Ω is most likely about 0.5(!). We emphasize that this is a preliminary analysis based on a small data set over a limited redshift range which will be substantially strengthened when our entire data set is in hand.

4. Conclusions. The CNOC cluster mapping project is designed to provide extensive dynamical data for a small sample of high X-ray luminosity clusters around $z \simeq 0.3$. The galaxies are observed with a technique of high velocity accuracy for the redshift range. The total random velocity errors are $\lesssim 150$ km s^{-1} of which only 100 km s^{-1} is due to velocity estimation, the rest being due to slit position and wavelength calibration uncertainties which potentially can be greatly reduced. The primary use of the data is to search for extended dark matter haloes around clusters, with a secondary application being to measure the value of the σ_8 normalization parameter for the amplitude of the density perturbation spectrum on cluster scales.

The data in hand, from a single telescope run of three clear nights in January 1993, are sufficient to put a new, fairly tight, limit on σ_8, confining it to the range of 0.6 to 0.9, using the volume density of high velocity dispersion clusters. The result is based on a cluster sample selected from an X-ray survey, which is insensitive to projection effects in sample construction and appears to be successful for finding rich, high velocity dispersion clusters.

A simple background decontamination technique has been developed which allows us to measure the extended mass profiles of clusters. The method has been applied to small samples of simulated data drawn from n-body simulations. For about 1000 cluster galaxies spread over half a dozen clusters, the method is sufficient to distinguish been the cluster M/L profiles characteristic of $\Omega = 0.2$ and $\Omega = 1$ universes, at a confidence level of 2–3 standard deviations.

At the present time we have about 230 redshifts, about ten per cent of the number that we need to complete this project to the accuracy necessary to get a statistically reliable result. The intent of this paper is to give a preliminary discussion of the overall goals of the project, the basic analysis procedures, and some tentative results.

Acknowledgements. We thank the CFHT Canadian Time Allocation Committee for a grant of observing time. CFHT staff, in particular Telescope Operators

Ken Barton, John Hamilton, and Norm Purvis, provided invaluable assistance at the telescope. The MOS team is to be congratulated for creating a superb instrument. Financial support for this project comes from the Natural Sciences and Engineering Research Council of Canada, the National Research Council, the Canadian Institute for Advanced Research, the Science and Engineering Research Council of the United Kingdom, the National Science Foundation and the National Aeronautics and Space Administration of the United States of America, and the Conseil National de Recherche Scientifique of France.

R.G. Carlberg,
Department of Astronomy,
University of Toronto,
60 St. George Street,
Toronto, Ontario,
M5S 1A7

References

Bahcall, J.N. & Tremaine, S. 1981, ApJ, 244, 805
Bardeen, J.M., Steinhardt, P.J. & Turner, M.S. 1983, Phys. Rev. D., 28, 679
Bean, A.J., Efstathiou, G., Ellis, R.S., Peterson, B.A. & Shanks, T. 1983, MNRAS, 205, 605
Bertschinger, E., Dekel, A., Faber, S.M., Dressler, A. & Burstein, D. 1990, ApJ, 364, 370
Bird, C.M. & Beers, T.C. 1993, AJ, 105, 1596
Bond, J.R. & Myers, S.T. 1992, in *Trends in Astroparticle Physics* (World Scientific: Singapore), p. 262
Bond, J.R. & Myers, S.T. 1993, ApJ, submitted
Carlberg, R.G. & Dubinski, J. 1991, ApJ, 369, 13
Carlberg, R.G. & Couchman, H.M.P. 1989, ApJ, 340, 47
Carlberg, R.G., Couchman, H.M.P. & Thomas, P.A. 1990, ApJLett, 352, L29
Crampton, D. *et al.* 1993, in *Proc. ESO Conference on Progress in Telescope and Instrumentation Technologies*, ed. M.-H. Ulrich (ESO: Garching) in press
Davis, M. & Peebles, P.J.E. 1983, ApJ, 267, 465
Davis, M., Efstathiou, G., Frenk, C.S. & White, S.D.M. 1985, ApJ, 292, 371
Edge, A.C., Stewart, G.C., Fabian, A.C., Arnaud, K.A. 1990, MNRAS, 245, 559
Edge, A.C. & Stewart, G.C. 1992, MNRAS, 252, 428
Efron, B. & Tishirani, R. 1986, *Statistical Science*, 1, 54
Efstathiou, G., Frenk, C.S., White, S.D.M. & Davis, M. 1988, MNRAS, 235, 715
Evrard, A.E. & Henry, J.P. 1991, ApJ, 383, 95
Frenk, C.S., White, S.D.M., Efstathiou, G.E. & Davis, M. 1990, ApJ, 351 10
Gioia, I.M., Maccacaro, T., Schild, R.E., Wolter, A., Stocke, J.T., Morris, S.L. & Henry, J.P. 1990, ApJSup, 72, 567
Guth, A.H. 1981, Phys. Rev. D., 23, 347
Henry, J.P., Gioia, I.M., Maccacaro, T., Morris, S.L., Stocke, J.T., & Wolter, A. 1992, ApJ, 386, 408
Huchra, J.P., Geller, M.J., Clemens, C.M., Tokarz, S.P., Michel, A. 1992, *The CfA Redshift Catalogue, "ZCAT"*, Bull. Inf. CDS 41, NASA NSSDC

Kaiser, N. 1991, ApJ, 383, 104
Kaiser, N., Efstathiou, G., Ellis, R., Frenk, C., Lawrence, A., Rowan-Robinson, M. & Saunders, W. 1991, MNRAS, 252, 1
Kent, S.M. & Gunn J.E. 1982, AJ, 87, 945
LeFèvre, O., Crampton, D., Felenbok, P., & Monnet, G. 1993, preprint
Merritt, D. 1987, ApJ, 313, 121
Morbey, C.L. 1992, *Applied Optics*, 31, 2291
Peebles, P.J.E. 1971, *Physical Cosmology*, Princeton University Press
Peebles, P.J.E. 1980, *The Large-Scale Structure of the Universe*, Princeton University Press
Peebles, P.J.E. 1993, *Principles of Physical Cosmology*, Princeton University Press
Press, W.H. & Schechter, P. 1974, ApJ, 187, 425
Saunders, W., Frenk, C., Rowan-Robinson, M., Efstathiou, G., Lawrence, A., Kaiser, N., Ellis, R., Crawford, J., Xia, X.-Y. & Parry, I. 1991, Nature, 349, 32
Smoot, G.F., Bennett, C.L., Kogut, A., Wright, E.L., Aymon, J., Boggess, N.W., Cheng, E.S., De Amici, G., Gulkis, S., Hauser, M.G., Hinshaw, G., Jackson, P.D., Jannsen, M., Kaita, E., Kelsall, T., Keegstra, P., Lineweaver, C., Lowenstein, K., Lubin, P., Mather, J., Meyer, S.S., Moseley, S.H., Murdock, T., Rokke, L., Silverberg, R.F., Tenorio, L., Weiss, R. & Wilkinson, D.T. 1992, ApJLett, 396, L1
Strauss, M.A., Yahil, A., Davis, M., Huchra, J.P. & Fisher, K. 1992, ApJ, 397, 395
The, L.S. & White, S.D.M. 1986, AJ, 92, 1248
van Haarlem, M., Coyon, L., Guitierrez de la Cruz, C., Martinez-Gonzalez, E., & Rebolo, R. 1993, MNRAS, 264, 71
West, M.J., & Richstone, D.O. 1988, ApJ, 335, 532
White, S.D.M. & Frenk, C.S. 1991, ApJ, 379, 52
White, S.D.M., Efstathiou, G., & Frenk, C.S. 1993, MNRAS, 262, 1023
Wright, E.L., Meyer, S.S., Bennett, C.L., Boggess, N.W., Cheng, E.S., Hauser, M.G., Kogut, A., Lineweaver, C., Mather, J.C., Smoot, G.F., Weiss, R., Gulkis, S., Hinshaw, G., Janssen, M., Kelsall, T., Lubin, P.M., Moseley, S.H. Jr., Murdock, T.L., Shafer, R.A., Silverberg, R.F. & Wilkinson, D.T. 1992, ApJLett, 396, L13.
Yee, H.K.C., *et al.* 1993, in preparation